Gait & Posture 108 (2024) 63–69

Contents lists available at ScienceDirect

Gait & Posture

journal homepage: www.elsevier.com/locate/gaitpost

Measuring highly accurate foot position and angle trajectories with foot-mounted IMUs in clinical practice

Andreas J. Jocham [a,*], Daniel Laidig [b,1], Bernhard Guggenberger [a,c,2], Thomas Seel [d,3]

[a] Institute of Physiotherapy, FH JOANNEUM University of Applied Sciences, Graz, Austria
[b] Control Systems Group, Technische Universität Berlin, Berlin, Germany
[c] Department of Orthopaedics and Trauma, Medical University of Graz, Graz, Austria
[d] Institute of Mechatronic Systems, Leibniz Universität Hannover, Hannover, Germany

ARTICLE INFO

Keywords:
Gait assessment
Inertial sensor
Foot-mounted
Digital health
Wearable sensor systems
Foot motion estimation

ABSTRACT

Background: Gait analysis using foot-mounted IMUs is a promising method to acquire gait parameters outside of laboratory settings and in everyday clinical practice. However, the need for precise sensor attachment or calibration, the requirement of environments with a homogeneous magnetic field, and the limited applicability to pathological gait patterns still pose challenges. Furthermore, in previously published work, the measurement accuracy of such systems is often only validated for specific points in time or in a single plane.
Research question: This study investigates the measurement accuracy of a gait analysis method based on foot-mounted IMUs in the acquisition of the foot motion, i.e., position and angle trajectories of the foot in the sagittal, frontal, and transversal plane over the entire gait cycle.
Results: A comparison of the proposed method with an optical motion capture system showed an average RMSE of 0.67° for pitch, 0.63° for roll and 1.17° for yaw. For position trajectories, an average RMSE of 0.51 cm for vertical lift and 0.34 cm for lateral shift was found. The measurement error of the IMU-based method is found to be much smaller than the deviations caused by the shoes.
Significance: The proposed method is found to be sufficiently accurate for clinical practice. It does not require precise mounting, special calibration movements, or magnetometer data, and shows no difference in measurement accuracy between normal and pathological gait. Therefore, it provides an easy-to-use alternative to optical motion capture and facilitates gait analysis independent of laboratory settings.

1. Introduction

The relevance of clinical gait analysis and the usefulness of objective data collection in the assessment of gait abnormalities has been discussed extensively over many years [1–3]. It has been shown that measurement of gait parameters is useful for both diagnosis and follow-up in different clinical fields [4–6]. Although marker-based optical motion capture (OMC) systems are considered the gold standard in motion analysis, their high accuracy can be accompanied by limitations, such as high cost, tedious execution, limited portability, laborious evaluation, and the need for line-of-sight between cameras and markers, which makes them challenging to use for some clinical purposes [2,7].

Low-cost wearable systems have therefore been discussed in recent years as a chance to provide access to instrumented gait analysis to a broader community and non-expert users and to facilitate its use independent from gait laboratories and in daily-life environments [8,9]. Gait analysis systems based on inertial measurement units (IMUs) have the potential to be used in such a manner [4]. Recently, various systems have been introduced, differing in the number and location of IMUs attached to the body. These range from single sensors on the pelvis, over two-sensor setups (one on each foot or shank), to more complex systems with a larger number of IMUs on different body segments [10]. However, the state of the art suffers from four main shortcomings.

(1) Different mathematical approaches are used to determine

* Correspondence to: Eggenberger Allee 13, 8020 Graz, Austria.
E-mail address: andreas.jocham@fh-joanneum.at (A.J. Jocham).
[1] Institutional address: Einsteinufer 17, 10587 Berlin, Germany
[2] Institutional address: Eggenberger Allee 13, 8020 Graz, Austria
[3] Institutional address: An der Universität 1, 30823 Garbsen, Germany

https://doi.org/10.1016/j.gaitpost.2023.11.002
Received 30 March 2023; Received in revised form 19 October 2023; Accepted 1 November 2023
Available online 4 November 2023

spatiotemporal parameters, gait phase durations, and trajectories [11]. Despite recent methodological advances [12,13], most IMU-based methods require precise attachment of the sensors or complex calibration procedures [14].

(2) Many studies have addressed the validity and reliability of IMU-based gait analysis systems in the acquisition of spatiotemporal parameters or kinematics, providing promising results [15]. Several studies investigated the accuracy of foot-mounted IMUs in estimating the position or angle of the feet during walking [16–26]. However, the results are often only presented for just one plane or direction [16–18,20,23–26], only at certain events in the gait cycle [16,22–24], or only at minimum or maximum values [21,22,26]. Showing the entire progression of foot positions and angles over time in the sagittal, frontal, and transversal plane, as it is common in OMC-based gait analysis [27], is highly desirable to get a deeper insight into the movement pattern.

(3) Furthermore, in some work [17,19,21,22,26], data is only collected from physiological gait, which limits the transferability of the results to clinical applications.

(4) In most research on IMU-based foot motion analysis [16–24,26], the sensors are attached to the shoes. This is expected, since IMU based systems enable gait analysis outside of laboratory settings in everyday life situations [4], which often requires the wearing of shoes. However, although relative motion between the sensor and the foot leads to measurement errors [25,28], this aspect is almost never investigated.

To address these four shortcomings, we consider the recently proposed method [29] for IMU-based gait analysis, which neither requires attachment in a precise orientation, specific calibration movements, nor magnetometer data. It has been demonstrated to yield highly accurate and robust gait phase durations and spatiotemporal parameters. We extend this method to also calculate foot position and angle trajectories. By only requiring one known sensor axis to lie in the sagittal plane pointing approximately forward, this extension makes minimal assumptions that are easy to achieve when mounting the IMU on the instep.

As the primary outcome, we validate those trajectories in sagittal, frontal, and transversal plane over the entire gait cycle during normal walking and induced limping. In contrast to previous research, we use an extended marker set and investigate the impact of sensor-to-shoe motion as the secondary outcome.

2. Methods

To address the research question, comparative measurements between the IMU-based gait analysis system and OMC were carried out in a motion analysis laboratory.

2.1. Participants

Twenty-three healthy volunteers (17 females, 6 males; age 24.8 ± 5.2 years, height 173.4 ± 8.9 cm, weight 67.2 ± 12.1 kg) participated in this study. Since comparable studies analysed data from 4 to 20 participants [16–26], a sample size of at least 20 participants was aimed for. The participants had to be capable of walking on a treadmill at different speeds and with simulated gait pathology. Exclusion criteria were current pain while walking or the presence of any disease that influences the gait pattern (e.g., due to orthopaedic or neurological conditions). All participants gave written informed consent prior to participation. The present study was approved by the Ethics Committee of the University of Graz (GZ. 39/55/63 ex 2017/18, 28 May 2018).

2.2. Instrumentation

One IMU (PABLO® Motion Sensor, Tyromotion GmbH, Graz, Austria) was attached on the instep of each shoe with three-point Velcro straps, shown in Fig. 1. Each sensor has a size of 56 × 34 × 21 mm, a weight of 40 g, and measures acceleration and angular rate with 110 Hz.

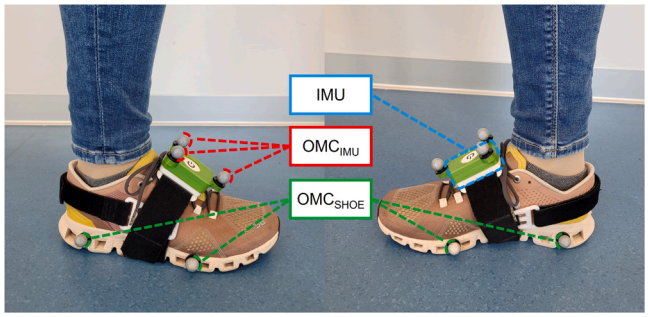

Fig. 1. IMU attached to a subject's shoe using Velcro strips and OMC markers attached to the sole of the shoe (OMC$_{SHOE}$) and, via a 3D printed console, to the IMU (OMC$_{IMU}$).

For all measurements, the same set of IMUs was used, with the identical sensors being attached to the left or right foot. An OMC system with 16 cameras (MX3, Vicon Inc., Oxford, UK) and a framerate of 120 Hz was used as reference. Three reflective markers were attached to a 3D printed console that was plugged onto the IMUs (OMC$_{IMU}$) and four on the edge of the sole of the subject's individual shoes (OMC$_{SHOE}$).

2.3. Procedure

Gait data were recorded simultaneously with IMUs and OMC while walking on a motorised treadmill (mercury® med, h/p/cosmos, Traunstein, Germany). Subjects were instructed to stand still with both feet side by side immediately before acceleration and after deceleration of the treadmill. The measurements were taken under four different conditions for 90 s each: very slow (1.5 km/h), slow (3 km/h), and normal walking speed (5 km/h), as well as with a simulated gait pathology at slow walking speed (3 km/h). To simulate gait pathologies, the range of motion of the subject's left knee joint was restricted with a brace fixed in neutral position. Prior to each trial, the subjects had time to get familiar with the respective condition. None of the participants chose to utilize the handrail of the treadmill.

2.4. Data processing

As the first processing step, the method described in [29] is applied to the IMU data. Among others, this outputs gait events, gait phase durations, and various spatiotemporal gait parameters. Separately for each foot, the following of those outputs are now used to derive the physiological foot position and angle trajectories illustrated in Fig. 2:

- the initial contact times $t_{ic,i}$ that mark the beginning of a new stride, and a rest time $t_{rest,i}$ in the middle of the foot-flat phase, for each stride i,
- an orientation quaternion $\mathbf{q}(t)$, representing the sensor orientation in an inertial reference frame $\mathscr{E}$ with vertical z-axis,
- a position trajectory $\mathbf{p}(t) = \begin{bmatrix} p_x & p_y & p_z \end{bmatrix}^T$, representing the sensor position in the reference frame $\mathscr{E}$.

To facilitate the derivation of physiological foot angles, sensor-to-foot alignment is performed, i.e., the relative orientation between the sensor coordinate system $\mathscr{S}$ and the foot coordinate system $\mathscr{F}$ (as illustrated in Fig. 2) is determined. To define this relative orientation, two axes of $\mathscr{F}$ need to be known in $\mathscr{S}$ coordinates. An estimate for the z-axis $\mathbf{z}_{\mathscr{F}}$ of the foot in sensor coordinates is obtained by averaging the accelerometer measurements during all foot-flat phases. Making use of the fact that the negative y-axis of the IMU points forward and down (due to the sensor attachment on the instep), the y-axis of the foot in sensor coordinates $\mathbf{y}_{\mathscr{F}}$ is given by $\mathbf{z}_{\mathscr{F}} \times \begin{bmatrix} 0 & -1 & 0 \end{bmatrix}^T$. Those two axes define the foot-to-sensor quaternion $\mathbf{q}_{\mathscr{F}\mathscr{S}}$, which is used to obtain the

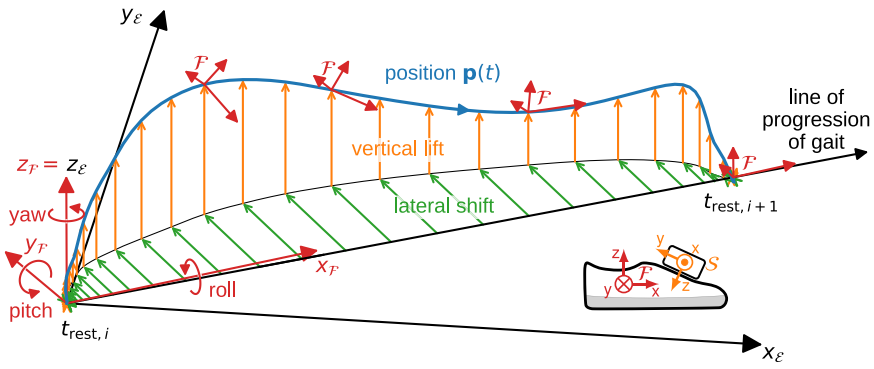

Fig. 2. Illustration of the foot coordinate system and position trajectories for an exemplary gait cycle of a left foot. The foot coordinate system $\mathcal{F}$ is defined with the x-axis pointing forward, the y-axis to the right, and the z-axis pointing up and, in general, different from the IMU coordinate system $\mathcal{S}$. The angles pitch, roll, and yaw are defined so that dorsal flexion, inversion, and out-toeing, respectively, are positive. (Notice the small amount of out-toeing at $t_{\text{rest},i}$.) The position trajectories lateral shift and vertical lift are defined based on the line of progression of gait. For illustration purposes, the displayed lateral shift and vertical lift are increased by a factor of 3.

orientation of the foot $\mathcal{F}$ relative to the reference frame $\mathcal{E}$: $\mathbf{q}_{\mathcal{EF}}(t) = \mathbf{q}(t) \otimes \mathbf{q}_{\mathcal{FS}}$.

Angles of the foot orientation relative to the reference frame are obtained by calculating intrinsic z-x'-y'' Euler angles of $\mathbf{q}_{\mathcal{EF}}$. The third angle, corresponding to the y''-axis, is called pitch, and the sign is inverted so that upward motion of the forefoot corresponds to a positive angle. The second angle (x') is roll. The sign is inverted for the left foot so that inversion corresponds to positive angles.

The first angle (z) is yaw. Since magnetometers are not used, the original yaw angle has an arbitrary offset. To obtain the foot progression angle (i.e., an angle that is zero when the x-axis of the foot points along the line of progression of gait), the line of progression of gait (cf. Fig. 2) is estimated from the position trajectory as $\text{atan2}\left(p_y\left(t_{\text{rest},i+1}\right) - p_y\left(t_{\text{rest},i}\right), p_x\left(t_{\text{rest},i+1}\right) - p_x\left(t_{\text{rest},i}\right)\right)$. This offset is removed from the original yaw angle. To ensure that out-toeing corresponds to positive angles, the sign is inverted for the right foot.

From the full 3D position $\mathbf{p}(t)$, two scalar position trajectories are derived: vertical lift and lateral shift. Vertical lift is defined as the vertical position of the IMU relative to the position during stance. Assuming level ground, a linear drift [29] is subtracted for each stride. The lateral shift is defined as the deviation of the position in the horizontal plane from the straight line of progression of gait.

As ground truth for comparison, analogous quantities are derived from the OMC marker positions. First, the IMU and OMC data is synchronized using the procedure described in [30]. Then, the sensor orientation is derived from the three markers attached to the IMU (OMC_{IMU}, cf. Fig. 1), and a sensor position trajectory is obtained by averaging the three marker positions. Further data processing is carried out analogously to the IMU data processing. Additionally, the same processing steps are applied to the foot orientation obtained from the four markers attached to the shoe (OMC_{SHOE}, cf. Fig. 1).

The angles (pitch, roll, and yaw) and positions (vertical lift and lateral shift) are then time-normalized based on the gait cycle. Fig. 3 shows an example over time for one subject. The gait cycle starts and ends at the initial contact, i.e., stride i occurs from $t_{\text{ic},i}$ (0 %) to $t_{\text{ic},i+1}$ (100 %). For each stride, the values are interpolated to a fixed length of 100 samples. The analysed trajectories and their standard deviations (SD) are obtained by calculating the mean and standard deviation of the gait-cycle-normalized quantities for each trial while excluding the first and last 5 strides.

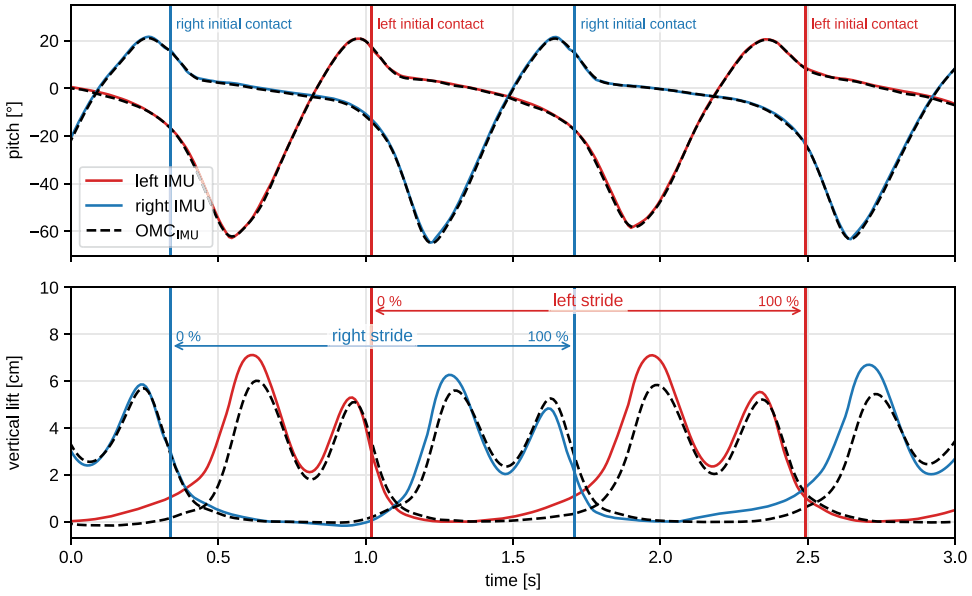

Fig. 3. Example for the pitch angle and vertical lift trajectories over two gait cycles of one subject. The vertical lines represent the initial contacts of the corresponding foot.

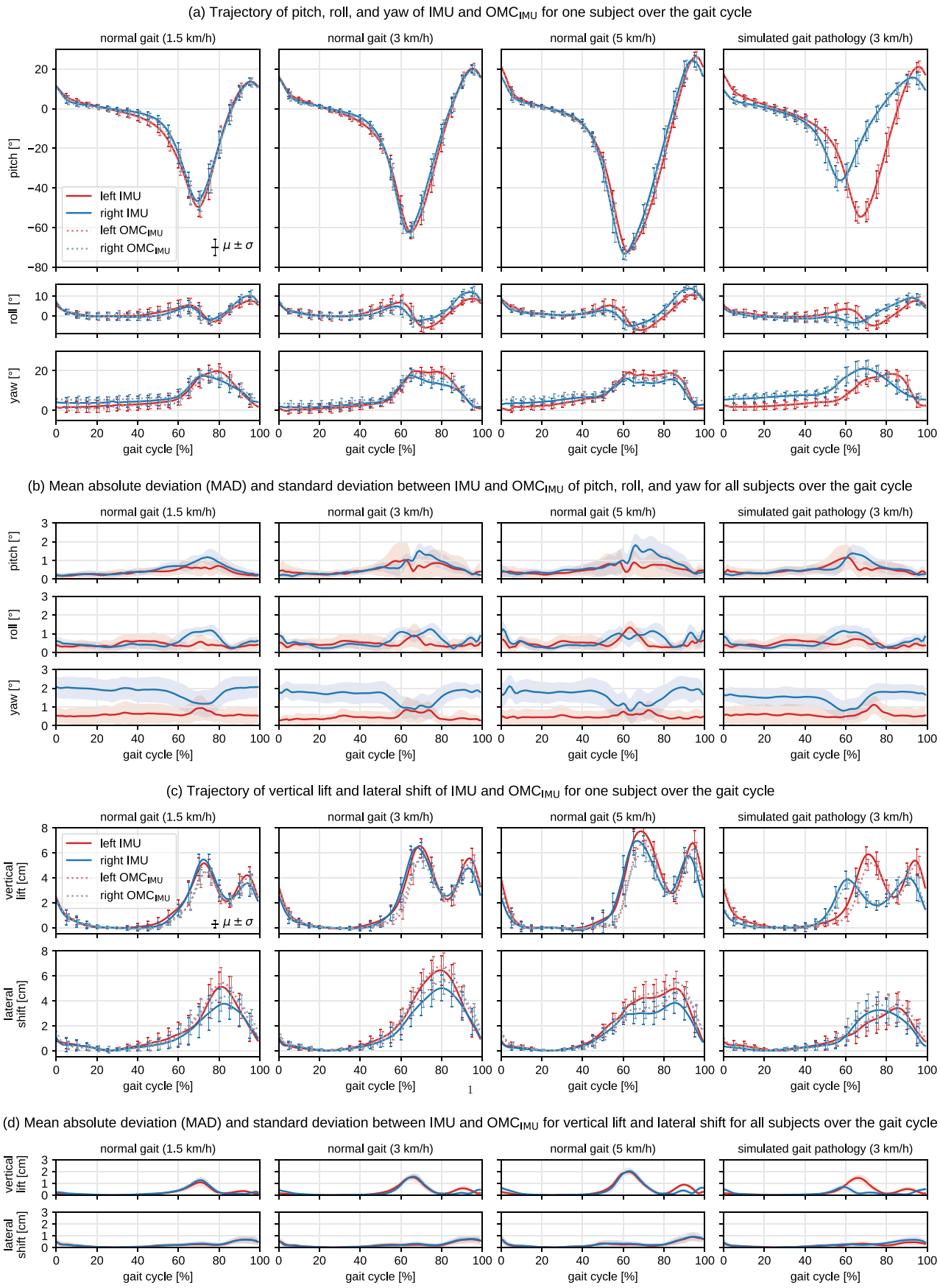

Fig. 4. : Time-normalized angle (a) and position (c) trajectories of one subject at different gait conditions. MAD between IMU and OMC$_{IMU}$ for angle (b) and position (d) trajectories of all subjects (n = 23).

3. Results

All recorded trials of all subjects were analysed, resulting in a total number of 9747 gait cycles (106 ± 30 gait cycles per trial). The average angle and position trajectories with SD for IMU and OMC_{IMU} for different walking conditions of one subject are presented in Fig. 4a and c, respectively. To compare the metrics for all subjects, the mean absolute difference (MAD) between the averaged gait-cycle-normalized IMU and OMC_{IMU} trajectories is shown in Fig. 4b and Fig. 4d. The maximum MAD occurs at a walking speed of 5 km/h and is 1.82° for pitch, 1.34° for roll, and 2.12° for yaw, as well as 2.04 cm for vertical lift and 0.94 cm for lateral shift. For each trial, the root mean square error (RMSE) between the IMU and OMC_{IMU} trajectories is presented as a boxplot in Fig. 5. The average RMSE of all trials is 0.67 ± 0.26° for pitch, 0.63 ± 0.19° for roll, 1.17 ± 0.69° for yaw, 0.51 ± 0.17 cm for vertical lift and 0.34 ± 0.15 cm for lateral shift. Finally, to evaluate the influence of the motion of the IMU relative to the shoe, the MAD between the IMU, OMC_{IMU} as well as OMC_{SHOE} for the angle trajectories is displayed in Fig. 6. It shows a maximum MAD between IMU and OMC_{SHOE} of 5.07° for pitch, 1.83° for roll, and 2.49° for yaw. In contrast, the maximum MAD between IMU and OMC_{IMU} is 0.97° for pitch, 0.86° for roll, and 1.21° for yaw.

4. Discussion

The aim of this study was to investigate the measurement accuracy of a gait analysis method based on foot-mounted IMUs in the acquisition of position and angle trajectories of the foot over the gait cycle as primary outcome. The results presented in Fig. 4 show good agreement between IMU and OMC_{IMU} for the position and angle trajectories. The differences between the systems are consistently low at all conditions, with a maximum MAD over the gait cycle for pitch, roll and yaw of about 2°, 2 cm for vertical lift, and 1 cm for lateral shift. The average RMSE for all parameters and all conditions is clearly below 1.5° and 1 cm, respectively, as shown in Fig. 5.

Comparing the results with those of other studies [16–26] that investigate the measurement accuracy of foot-mounted IMUs for positions and angles is only possible to a limited extent, since samples, measurement protocols, and evaluated parameters differ considerably between studies. However, it can be stated that the measurement error of the presented method for angle trajectories is comparable to other publications [17,19,20,22,23] or even lower [16,18,24,25]. The measurement error for position trajectories is comparable [21,22] or lower [17,19,26]. In contrast to [17,18,24], in which gait deviations were also simulated by healthy participants, the results for the trials with provoked limping do not show a deterioration of accuracy. This observation coincides with the findings of [29], in which the presented method was shown to provide comparable results for healthy subjects and patients

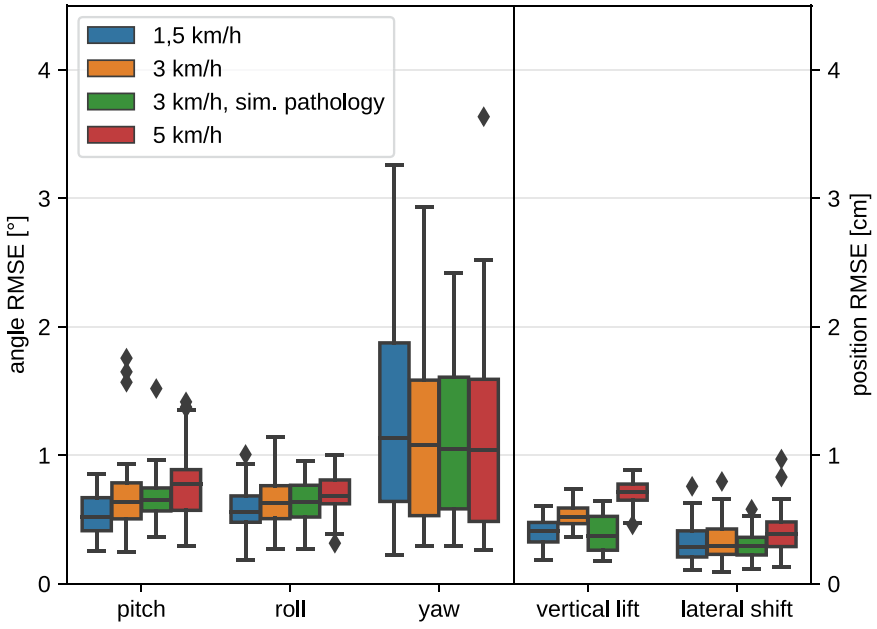

Fig. 5. RMSE between IMU and OMC_{IMU} for angle and position trajectories of all subjects (n = 23) at different gait conditions.

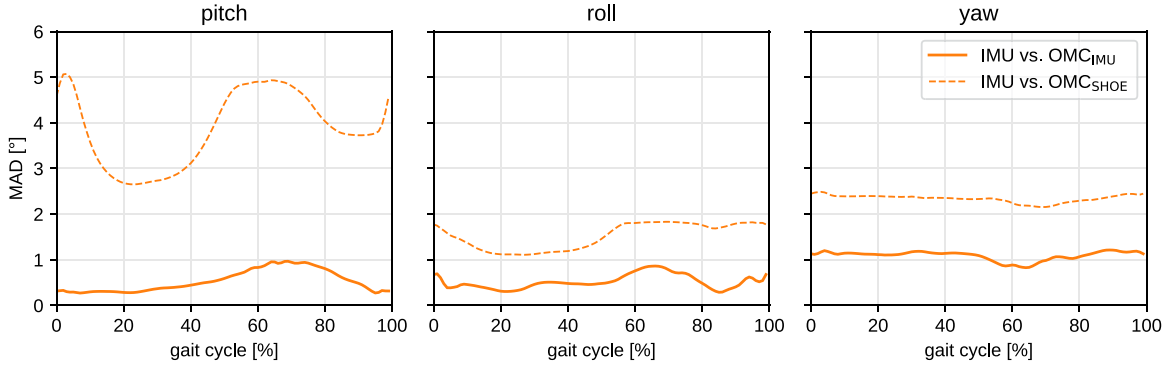

Fig. 6. Time-normalized trajectories of the MAD between IMU and OMC_{IMU} as well as IMU and OMC_{SHOE} of all subjects (n = 23) and all 62 trials.

with different gait deviations.

In future work, the accuracy in acquisition of position and angle trajectories of the presented method should be investigated with patients with various gait pathologies and for overground walking.

The proposed method provides foot trajectories displayed as time-normalized graphs over the gait cycle for sagittal, frontal, and transversal plane. For clinicians, this visualization contains valuable information for the assessment of gait deviations. The presented approach enables a deeper understanding of the evaluated gait pattern compared to minimum and maximum values [21,22,26] or values at certain events in the gait cycle [16,22–24]. For example, the pitch angle during initial contact could be used to assess drop foot after stroke and the associated increased risk of falls [31]. The position and angle trajectories in the sagittal, frontal, and transversal plane provide further information about associated gait deviations, e.g., circumduction, and, beyond that, even enables visualisation of the entire foot motion in 3D space. Furthermore, this method could be used for the objective evaluation of aids, such as ankle foot orthoses. The deviations (e.g. drop foot, circumduction) associated with pathologies as stroke, which is often treated by such aids, typically exhibit magnitudes in the range 3–10 cm [32] and 5–20° [33–36]. The proposed method is accurate enough to detect such changes. Furthermore, it makes IMU-based gait analysis practical since no precise alignment and no specific calibration movements or magnetometer data are required [29].

In many studies [16–24,26] investigating positions or angles with foot-mounted IMUs, the sensors were attached to the outside of the shoe, except for [23], which includes additional barefoot measurements. In all those studies, OMC was used as ground truth, with some placing the markers on the IMU [16–18,21,22], others on the shoe [19,23–26] or both [20]. However, none of these publications investigated the influence of the shoe on the results.

Therefore, the influence of shoe motion was investigated as a secondary outcome. In this context, the present setup with both OMC_{IMU} and OMC_{SHOE} yields new findings. As shown in Fig. 6, the MAD between IMU and OMC_{IMU} is considerably smaller than between IMU and OMC_{SHOE} for all angle trajectories. This shows that the impact of OMC marker placement on the obtained measurement is as large or even larger than the disagreements between OMC and IMU-based measurements. This should be considered when interpreting the data, especially for gait deviations where the position of the shoe sole is highly relevant (e.g., limited ground clearance during swing phase).

In future work, it should be clarified which sensor position and mounting on the shoe results in the lowest measurement error. The common practice of attaching foot-mounted IMU systems to shoes should be viewed critically overall. In clinical use, it must be considered whether the advantage of easy-to-use gait analysis in everyday situations outweighs the disadvantage of less accurate results caused by the shoe.

A limiting factor of this work is that the data were only collected from healthy subjects. However, the applied simulated gait pathology affected the swing phase comparable to a knee extension contracture, leading to significant differences in the movement pattern between the left and right side (cf. Fig. 4). Furthermore, the provoked functional leg length difference in the swing phase led to known compensatory mechanisms described in the literature, such as circumduction, contralateral vaulting, or pelvic hike [3].

The data were collected while walking on a treadmill. This approach was chosen to avoid the subjects having to leave the OMC recording area and thus to enable continuous measurements. In addition, reducing the imaging volume via repositioning of the OMC cameras provided better detection and differentiation of the optical markers.

As a minor observation, Fig. 4 shows a slightly larger MAD for the right yaw angle due to an offset that is likely caused by inaccurate factory calibration of the right IMU.

A limitation in the detection of OMC_{SHOE} is the fact that the subjects were examined with their individual shoes. The differences in the shape and flexibility of the sole should be considered when interpreting these results.

5. Conclusions

In summary, the presented method can determine position and angle trajectories with a promising consistency between IMU and OMC. In contrast to other works, no differences in measurement accuracy between normal walking and pathological movement patterns occurred. Furthermore, it is shown that the measurement error of the IMU itself is significantly lower than that caused by the shoes. The proposed method is found to be sufficiently accurate for clinical practice. It neither requires attachment in a precise orientation, nor specific calibration movements, nor magnetometer data. Gait analysis systems based on foot-mounted IMUs are a viable alternative to OMC, enabling comprehensive gait analysis in everyday clinical practice that is not restricted to laboratory environments or predefined walking paths.

Declaration of Competing Interest

The authors declare the following financial interests/personal relationships which may be considered as potential competing interests: A. J. Jocham was employed by Tyromotion GmbH (Graz, Austria) prior to data collection for this work. Other authors declare no conflict of interest.

Acknowledgements

The authors would like to thank all participants for their participation in the study.

References

[1] R. Baker, Gait analysis methods in rehabilitation, J. Neuroeng. Rehabil. 3 (1) (2006) 4, https://doi.org/10.1186/1743-0003-3-4.
[2] S.R. Simon, Quantification of human motion: gait analysis—benefits and limitations to its application to clinical problems, J. Biomech. 37 (12) (2004) 1869–1880, https://doi.org/10.1016/j.jbiomech.2004.02.047.
[3] J. Perry, J.M. Burnfield, Eds., Gait analysis: normal and pathological function, 2. ed. Thorofare, NJ: SLACK, 2010.
[4] S. Chen, J. Lach, B. Lo, G.-Z. Yang, Towards pervasive gait analysis with wearable sensors: a systematic review, 14, 8, p. 18, 2016.
[5] R. Baker, A. Esquenazi, M.G. Benedetti, K. Desloovere, Gait analysis: clinical facts, Eur. J. Phys. Rehabil. Med. 52 (4) (2016) 560–574.
[6] S. Nadeau, M. Betschart, F. Bethoux, Gait analysis for poststroke rehabilitation, Phys. Med. Rehabil. Clin. N. Am. 24 (2) (2013) 265–276, https://doi.org/10.1016/j.pmr.2012.11.007.
[7] E. van der Kruk, M.M. Reijne, Accuracy of human motion capture systems for sport applications; state-of-the-art review, Eur. J. Sport Sci. 18 (6) (2018) 806–819, https://doi.org/10.1080/17461391.2018.1463397.
[8] W. Tao, T. Liu, R. Zheng, H. Feng, Gait analysis using wearable sensors, Sensors 12 (2) (2012) 2255–2283, https://doi.org/10.3390/s120202255.
[9] M. Iosa, P. Picerno, S. Paolucci, G. Morone, Wearable inertial sensors for human movement analysis, Expert Rev. Med. Devices 13 (7) (2016) 641–659, https://doi.org/10.1080/17434440.2016.1198694.
[10] F. Petraglia, L. Scarcella, G. Pedrazzi, L. Brancato, R. Puers, C. Costantino, Inertial sensors versus standard systems in gait analysis: a systematic review and meta-analysis, Eur. J. Phys. Rehabil. Med. 55 (2) (2019), https://doi.org/10.23736/S1973-9087.18.05306-6.
[11] R. Caldas, M. Mundt, W. Potthast, F. Buarque de Lima Neto, B. Markert, A systematic review of gait analysis methods based on inertial sensors and adaptive algorithms, Gait Posture 57 (2017) 204–210, https://doi.org/10.1016/j.gaitpost.2017.06.019.
[12] T. Seel, M. Kok, R.S. McGinnis, Inertial sensors—applications and challenges in a nutshell, Sensors 20 (21) (2020) 6221, https://doi.org/10.3390/s20216221.
[13] B. Taetz, G. Bleser, and M. Miezal, Towards self-calibrating inertial body motion capture.
[14] K. Berner, J. Cockcroft, L.D. Morris, Q. Louw, Concurrent validity and within-session reliability of gait kinematics measured using an inertial motion capture system with repeated calibration, J. Bodyw. Mov. Ther. 24 (4) (2020) 251–260, https://doi.org/10.1016/j.jbmt.2020.06.008.
[15] D. Kobsar, et al., Validity and reliability of wearable inertial sensors in healthy adult walking: a systematic review and meta-analysis, J. Neuroeng. Rehabil. 17 (1) (2020) 62, https://doi.org/10.1186/s12984-020-00685-3.
[16] A. Brégou Bourgeois, B. Mariani, K. Aminian, P.Y. Zambelli, C.J. Newman, Spatio-temporal gait analysis in children with cerebral palsy using, foot-worn inertial

sensors, Gait Posture 39 (1) (2014) 436–442, https://doi.org/10.1016/j.gaitpost.2013.08.029.
[17] M. Benoussaad, B. Sijobert, K. Mombaur, C. Azevedo Coste, Robust foot clearance estimation based on the integration of foot-mounted IMU acceleration data, Sensors 16 (1) (2015) 12, https://doi.org/10.3390/s16010012.
[18] E. Chalmers, J. Le, D. Sukhdeep, J. Watt, J. Andersen, E. Lou, Inertial sensing algorithms for long-term foot angle monitoring for assessment of idiopathic toe-walking, Gait Posture 39 (1) (2014) 485–489, https://doi.org/10.1016/j.gaitpost.2013.08.021.
[19] J. Hannink, M. Ollenschläger, F. Kluge, N. Roth, J. Klucken, B.M. Eskofier, Benchmarking foot trajectory estimation methods for mobile gait analysis, Sensors 17 (9) (2017) 1940, https://doi.org/10.3390/s17091940.
[20] Y. Huang, W. Jirattigalachote, M.R. Cutkosky, X. Zhu, P.B. Shull, Novel foot progression angle algorithm estimation via foot-worn, magneto-inertial sensing, IEEE Trans. Biomed. Eng. 63 (11) (2016) 2278–2285, https://doi.org/10.1109/TBME.2016.2523512.
[21] N. Kitagawa, N. Ogihara, Estimation of foot trajectory during human walking by a wearable inertial measurement unit mounted to the foot, Gait Posture 45 (2016) 110–114, https://doi.org/10.1016/j.gaitpost.2016.01.014.
[22] B. Mariani, C. Hoskovec, S. Rochat, C. Büla, J. Penders, K. Aminian, 3D gait assessment in young and elderly subjects using foot-worn inertial sensors, J. Biomech. 43 (15) (2010) 2999–3006, https://doi.org/10.1016/j.jbiomech.2010.07.003.
[23] F.J. Wouda, S.L.J.O. Jaspar, J. Harlaar, B.-J.F. van Beijnum, P.H. Veltink, Foot progression angle estimation using a single foot-worn inertial sensor, J. Neuroeng. Rehabil. 18 (1) (2021) 37, https://doi.org/10.1186/s12984-021-00816-4.
[24] H. Schwameder, M. Andress, E. Graf, G. Strutzenberger, Validation of an IMU-system (Gait-Up) to identify gait parameters in normal walking and induced limping wakling conditions, p. 4, 2015.
[25] T. Seel, D. Graurock, T. Schauer, Realtime assessment of foot orientation by accelerometers and gyroscopes, Curr. Dir. Biomed. Eng. 1 (1) (2015) 446–469, https://doi.org/10.1515/cdbme-2015-0112.
[26] B. Mariani, S. Rochat, C.J. Büla, K. Aminian, Heel and toe clearance estimation for gait analysis using wireless inertial sensors, IEEE Trans. Biomed. Eng. 59 (11) (2012) 3162–3168, https://doi.org/10.1109/TBME.2012.2216263.
[27] R. Baker, Measuring Walking: A Handbook of Clinical Gait Analysis, Mac Keith Press, London, 2013.
[28] A.R. Anwary, H. Yu, M. Vassallo, Optimal foot location for placing wearable imu sensors and automatic feature extraction for gait analysis, IEEE Sens. J. 18 (6) (2018) 2555–2567, https://doi.org/10.1109/JSEN.2017.2786587.
[29] D. Laidig, A.J. Jocham, B. Guggenberger, K. Adamer, M. Fischer, T. Seel, Calibration-free gait assessment by foot-worn inertial sensors, Front. Digit. Health 3 (2021), 736418, https://doi.org/10.3389/fdgth.2021.736418.
[30] D. Laidig, M. Caruso, A. Cereatti, T. Seel, BROAD—a benchmark for robust inertial orientation estimation, Data 6 (7) (2021) 72, https://doi.org/10.3390/data6070072.
[31] F. Feuvrier, et al., Inertial measurement unit compared to an optical motion capturing system in post-stroke individuals with foot-drop syndrome, Ann. Phys. Rehabil. Med. 63 (3) (2020) 195–201, https://doi.org/10.1016/j.rehab.2019.03.007.
[32] N. Itoh, et al., Quantitative assessment of circumduction, hip hiking, and forefoot contact gait using Lissajous figures, Jpn. J. Compr. Rehabil. Sci. 3 (0) (2012) 78–84, https://doi.org/10.11336/jjcrs.3.78.
[33] L. Zollo, et al., Comparative analysis and quantitative evaluation of ankle-foot orthoses for foot drop in chronic hemiparetic patients, Eur. J. Phys. Rehabil. Med. 51 (2) (2015).
[34] J. Ernst, et al., Towards physiological ankle movements with the ActiGait implantable drop foot stimulator in chronic stroke, Restor. Neurol. Neurosci. 31 (5) (2013) 557–569, https://doi.org/10.3233/RNN-120283.
[35] T. Seel, D. Laidig, M. Valtin, C. Werner, J. Raisch, T. Schauer, Feedback control of foot eversion in the adaptive peroneal stimulator, in 22nd Mediterranean Conference on Control and Automation, Palermo, Italy: IEEE, Jun. 2014, pp. 1482–1487. doi: 10.1109/MED.2014.6961585.
[36] Y.-I. Hwang, D.-J. Park, Effects of elastic neutral ankle-foot orthoses on 3 dimensional parameters during gait training in patients with stroke: a pilot study, J. Bodyw. Mov. Ther. 27 (2021) 300–306, https://doi.org/10.1016/j.jbmt.2021.02.008.